Neural Computing and Applications (2020) 32:8829–8846
https://doi.org/10.1007/s00521-019-04354-y

ORIGINAL ARTICLE

Efficiency of optimization algorithms on the adjustment of process parameters for geometric accuracy enhancement of denture plate in single point incremental sheet forming

Manel Sbayti[1] · Riadh Bahloul[1] · Hedi Belhadjsalah[1]

Received: 24 April 2018 / Accepted: 18 July 2019 / Published online: 7 August 2019

Abstract
Single point incremental forming is a sheet metal forming technique with great potential for use in prototyping and custom manufacture. Although this technology has undergone considerable development in recent years, it still suffers from low geometrical accuracy in terms of its application in the industry. Therefore, solutions for errors reduction or compensation are required to improve the process. In this paper, an optimization procedure of the geometric precision, based on genetic algorithm, global optimum determination by linking and interchanging kindred evaluators solver and newly developed algorithm called grasshopper optimization algorithm, is tested and doubly validated numerically and experimentally. The denture plate part simultaneously simulated and manufactured shows how it is possible to obtain sound component with reduced geometric errors such as springback, bending and pillow effect errors by properly chosen optimal process parameters. The results indicated that the reduction in the shape defects between the obtained geometry and the target model generated by computer-aided design can be achieved through coupling of numerical simulations and optimization techniques.

Keywords Single point incremental forming · Denture plate · Geometric accuracy · GA · GODLIKE · GOA

Abbreviations

ISF	Incremental sheet forming
SPIF	Single point incremental forming
CAD/CAM	Computer-aided design/computer-aided manufacturing
DICOM	Digital image and communications in medicine
CT	Computerized tomography
PCL	Polycaprolactone
MARS	Multivariate adaptive regression splines
MPC	Model predictive control
RSM	Response surface methodology
FE	Finite element
DoE	Design of the experiments
BBD	Box–Behnken design of experiments
ANOVA	Analysis of variance
GAs	Genetic algorithms
MaxGen	Maximum number of generations
GODLIKE	Global optimum determination by linking and interchanging kindred evaluators
POF	Pareto optimal frontier
GA	Genetic algorithm
DE	Differential evolution
PSO	Particle swarm optimization
ASA	Adaptive simulated annealing
GOA	Grasshopper optimization algorithm
SOOP	Single-objective optimization problems
MOOP	Multi-objective optimization problems
MOGA	Multi-objective genetic algorithm

✉ Hedi Belhadjsalah
hedi.belhadjsalah@enim.rnu.tn;
hedi.belhadjsalah1@gmail.com

Manel Sbayti
manelasbayti@gmail.com

Riadh Bahloul
bahloul_riadh@yahoo.fr

[1] Laboratory of Mechanical Engineering (LGM), National Engineering School of Monastir (ENIM), University of Monastir, Av. Ibn El Jazzar, 5000 Monastir, Tunisia

1 Introduction

Cost-effective technologies suitable for prototyping, customized components and small batch production represent a challenge for the actual market [1]. The answer to these

requirements are the flexible, time and cost-saving manufacturing process as rapid prototyping and, in particular, incremental sheet forming (ISF) seems to be the most effective and reliable one when referring to prototypes, small batch and customized mass productions [2–4]. Without using dedicated dies, parts are formed by the motion of a small hemispherical end tool traveling along a 3D CAM toolpath on the surface of the sheet wherein a localized deformation will be generated [5, 6].

This technology was primarily applied in the automobile and aerospace industry [7, 8]. However, there are other branches with an important potential for the technology, such as the biomedical field [9]. When addressing its use in medicine, it is possible to produce thin walled custom-made metal components. When addressing its use in medicine, it is possible to produce thin walled custom-made metal components. Araújo et al. [10] demonstrated the feasibility of single point incremental forming process (SPIF) to produce titanium customized maxillofacial implants. Castelan et al. [11] presented the manufacturing by ISF of the custom-made cranial implants from a sheet of pure grade 2 titanium from digital image and communications in medicine (DICOM) images using 3D printing, CAD/CAM technology and incremental sheet forming. From computerized tomography (CT) images of a fractured skull, a CAD model of the skull BioModeling and a restorative implant were constructed digitally. Duflou et al. [12] used three different materials: AA1050, AISI 304 and medical grade titanium for accurate manufacture of craniofacial implant using SPIF process. Fiorentino et al. [13] manufactured a plate prosthesis using a titanium alloy and polycaprolactone (PCL). Although their results were promising, the poor accuracy of the part needs an optimization of the process parameters. While there has been much discussion of SPIF as a useful custom manufacturing process, only a small number of end user ready applications have been documented. Nevertheless, the big advantages connected with this technology, there are some critical aspects related to the part feasibility and the part precision. For any process to be widely adopted, one must be able to clearly communicate to the end users the capabilities and limitations. To achieve this, the main limit of the technology represented by the geometrical errors that can be found on the final shape [14] should be overcome.

In order to improve the poor geometrical accuracy, some attempts have been presented in the literature, including experimental investigation of process parameters [15, 16], hybrid ISF processes [17–19], the use of partially cutout blanks [20] and a multistage strategy [21]. Moreover, since the adopted toolpath greatly influences thinning and feasibility, many studies concentrated on the toolpath correction/optimization. The ISF toolpath can be corrected by using error compensation based on trial fabrications [5], a feature-based toolpath generation strategy [22], a multivariate adaptive regression splines (MARS) correction strategy [23], iterative algorithms [24–26], transfer function [27] and an artificial cognitive system [28]. Moreover, some in-process toolpath correction approaches were performed in SPIF based on a control strategy using spatial impulse responses of the process [29] and a model predictive control (MPC) strategy [30, 31]. Some research has been performed to reduce the main drawbacks of ISF process with new approaches for optimization problems based on numerical simulation, response surface methods (RSM) and genetic algorithms [32, 33].

Within a so wide panorama of issues to be considered for obtaining a sound part through ISF, the use of preliminary finite element (FE) tools is of great help in reducing time and cost for the design of the manufacturing process [34–36]. In our previous work [37], the feasibility of manufacturing customized titanium denture plate by using the ISF approach has been studied within the frame of a preliminary optimization procedure by evaluating multi-objective optimization methods for SPIF process parameters. Nevertheless, good adequacy has been proved between the optimized process parameters, the SPIF finite element simulation and the obtained experimental part. Geometric accuracy is still the critical aspect to be corrected especially the sheet springback [38], the sheet bending [39] and the "pillow effect" (known as an unwanted curved surface, typically occurs on the flat base of the part formed by SPIF) [40]. The results showed that the incremental forming process was a new process where there remains room for improvement toward limited dimensional precision.

Besides that the computer science [41–44] is one of the most developing and in demand trades of engineering. Its fast growth and development [45–48] have a beneficial impact on the manufacturing industry [49].

For this reason, this article proposes the use of a parameterized FE model and optimization procedure to reduce these process limitations: springback error, bending error and pillow effect error. This technique will also lead to reduce time and materials consuming compared to others methods which are generally based on several experimental tests combined with normalized techniques [50–52].

2 Numerical modeling and design procedure of computer experiments

2.1 Framework of the proposed method

Based on the experimental results of incremental sheet forming process shown in our previous work [37], obvious geometric errors have been noted. This is the major well-known limitation of SPIF process. Therefore, this study

aims to reduce theses errors. The virtual process chain for the simulation-based development of Pareto-optimized SPIF process responses is presented in Fig. 1. The design optimization starts with the design of the experiments (DoE) that leads to perform the simulation study. For this, a parameterized FE model of SPIF process is used. During the post-processing of each single simulation, the considered target responses expressed in terms of the final geometry of the parts are evaluated and recorded. The DoE design and the calculated geometric errors are then used to derive a metamodel to reduce the computational cost during the design optimization. The last step of the design optimization sub-process consists in finding the optimal design variables for the optimization problem of incremental forming by applying mono- and multi-objective optimization methodologies with regard to one or more target figures. Then, the attained optimal solution and the optimal process parameters are used to make an experimental validation test for the manufacture of the titanium denture plate. Finally, the geometry of the part obtained with experimental measurement has been compared to the desired one in order to verify the efficacity of the used procedure. Each process step depicted in Fig. 1 will be described in the following sections in more detail.

2.2 Numerical simulation of SPIF process

Due to the cost materials and time for the experimental study, it is necessary to build the FE model to conduct the simulation analysis and realize the virtual that reflect the actual situation exactly. Based on the scanned shape of an existing custom-made denture base, the toolpath has been generated to produce simultaneously two identical denture base parts (Fig. 2). The shape of the titanium sheet has been considered square with a size of 120 mm × 120 mm. The sheet was clamped into a fixed rectangular blank holder, and a backing plate is placed underneath it to support the part. In the FE model, A 4-node doubly curved thin or thick shell (S4R) and seven Gaussian reduced integration points through the thickness direction were used to model the sheet blank with approximately 14.400 elements. The rig and the clamp are meshed with 4-node 3-D bilinear rigid quadrilateral elements (R3D4). The punch is supposed to be analytical rigid surface. The sheet material used in the numerical simulation is CP-Ti Gr.1. It was modeled as an elasto-plastic material with isotropic hardening. The material properties of CP-Ti Gr.1 pure titanium are taken from [9]. As a result, the FE model of the SPIF can be obtained as shown in Fig. 3 using

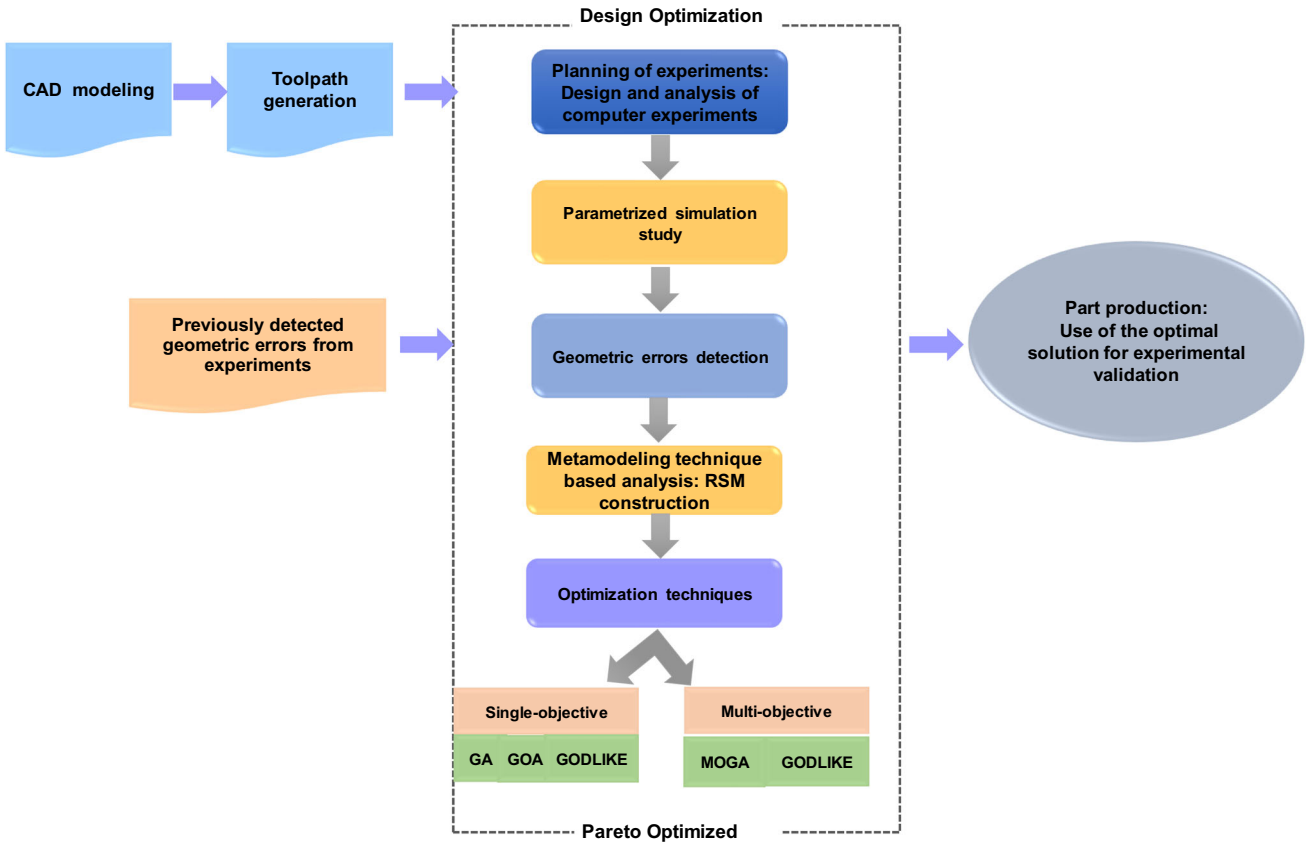

Fig. 1 Flowchart of the optimization procedure for geometric errors reduction in SPIF process

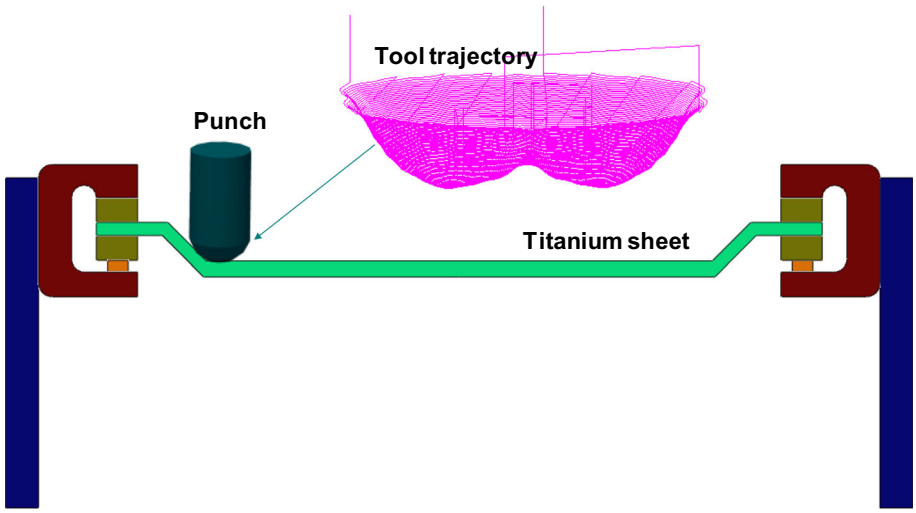

Fig. 2 SPIF process principle

ABAQUS–Explicit software package. As shown in Fig. 4, the geometric errors between the theoretical profile provided by CAD modeling and the one obtained with numerical simulation have been calculated in three critical areas: the springback zone, the bending zone and the pillow effect zone.

2.3 Design of experiments

For this study, a parameterized FE model has been developed. Therefore, the process parameters and their levels to be used in the simulation study have been chosen based on experimental design. Design of experiments (DoE) is a cost-effective tool for controlling the influence of parameters in manufacturing processes. The selection of a suitable DoE with respect to a compromise between high accuracy and limited time to carry out the experiment is crucial at the beginning of a DoE process. In order to reduce the factors combinations, and therefore the overall time to carry out the simulation study, Box–Behnken Designs (BBD) [53] was chosen. The target process responses of interest in this contribution are the geometric errors measured between obtained and desired cad part in three areas: the springback zone, the bending zone and the pillow effect zone. Therefore, a total number of 15 numerical simulation runs will be needed for the development of an adequate geometric errors prediction models by finding out the relationship between the response functions and the variables (tool diameter, vertical increment size and friction coefficient). The considered parameters and their levels are, respectively: tool diameter (D: 5, 7.5, 10 mm), step down (Δz: 0.02, 0.11, 0.2 mm) and friction coefficient (μ: 0.05, 0.15, 0.25). The main objective of this procedure is to define the most critical process parameters and their effect on the considered responses for denture plate manufacturing. Table 1 summarizes the matrix of experiments which represents the process parameters combinations and the SPIF studied responses obtained by the previously described numerical simulation.

3 Response surface methodology

Response surface methodology (RSM) is a statistical model, frequently used to analyze, evaluate, predict and/or optimize a response variable that is influenced by some

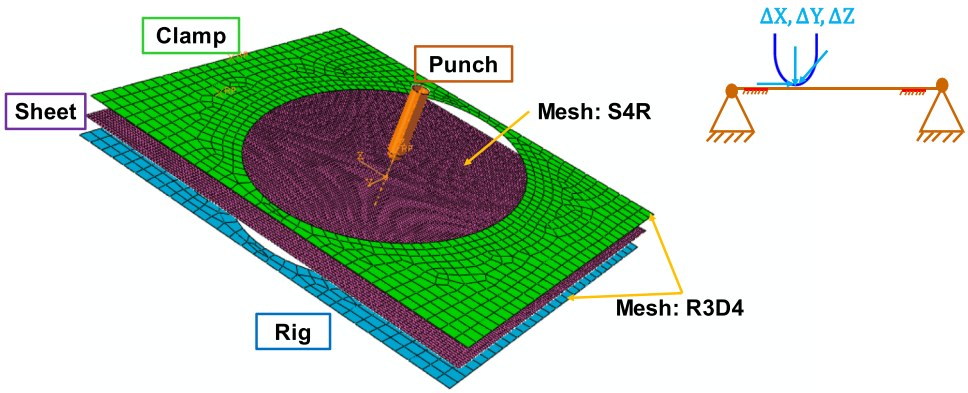

Fig. 3 Simulation principle of SPIF process

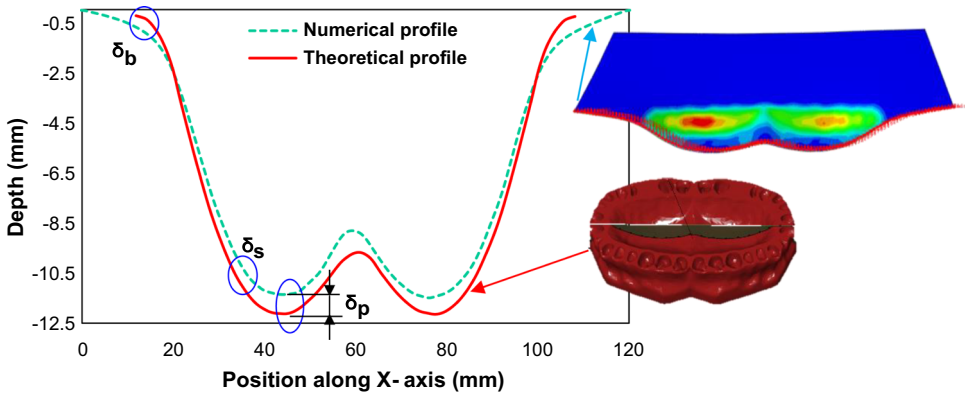

Fig. 4 Comparison of geometric errors predicted by FE simulation with theoretical geometrical model generated by computer-aided design (CAD)

Table 1 Box–Behnken design of experiments matrix with three independent variables and responses

Run no.	D	Δz	μ	Bending error	Pillow effect error	Springback error
1	10	0.2	0.15	0.949068	0.691896	0.841086
2	10	0.11	0.25	0.837698	0.656196	0.675086
3	7.5	0.2	0.05	0.442568	0.808196	0.267386
4	7.5	0.11	0.15	0.375448	0.957396	0.700586
5	7.5	0.11	0.15	0.375448	0.957396	0.700586
6	7.5	0.02	0.25	0.604702	0.596596	0.2
7	5	0.02	0.15	0.086762	0.656896	0.267386
8	7.5	0.11	0.15	0.375448	0.957396	0.700586
9	10	0.02	0.15	0.887788	0.004896	0.536986
10	7.5	0.2	0.25	0.538678	0.797996	0.711886
11	10	0.11	0.05	0.841298	0.648096	0.660386
12	5	0.11	0.25	0.378458	0.801396	0.778786
13	7.5	0.02	0.05	0.459532	0.447696	0.322686
14	5	0.11	0.05	0.442388	0.787196	0.784386
15	5	0.2	0.15	0.574248	0.820396	1.210786

decision or independent variables [54, 55]. After identifying some vital controllable factors, the RSM model can be applied to find values of various process parameters that optimize the response variable and can also be used to predict the desired response according to those independent factors. RSM analysis includes the formation of a regression equation using the relationship between the response and independent variables which helps to determine a mathematical correlation and the influence of interactions of different independent variables on the corresponding response [56]. In the presence of complicated relationships between the input variables and output responses, the most significant factors influencing a physical response of such process can also be determined through the application of variance analysis (ANOVA) [57]. Consider a response y that is determined as a function of variable X_i, the second order polynomial regression model (full quadratic model) can be represented by Eq. (1):

$$y = \beta_0 + \sum_{i=1}^{k} \beta_i X_i + \sum_{i=1}^{k} \beta_{ii} X_i^2 + \sum_{kj} \sum \beta_{ij} X_i X_j + \varepsilon \quad (1)$$

where k is the number of design variables, X_i is the set of design variables, β_i are the polynomial coefficients, and ε is minor error.

In our case, the regression equations defining the SPIF process responses in terms of bending error $(\boldsymbol{\delta_b})$, pillow effect error $(\boldsymbol{\delta_p})$ and springback error $(\boldsymbol{\delta_s})$ could be summarized as follows:

$$\begin{aligned}\delta_b = {} & 1.050 - 0.290\,D + 2.56\,\Delta z - 2.13\,\mu + 0.0290\,D \\ & \times D + 8.36\,\Delta z \times \Delta z + 6.82\,\mu \times \mu - 0.474\,D \\ & \times \Delta z + 0.060\,D \times \mu - 1.36\,\Delta z \times \mu\end{aligned} \quad (2)$$

$$\begin{aligned}\delta_p = {} & -0.563 + 0.308\,D + 4.71\,\Delta z + 2.46\,\mu - 0.02826\,D \\ & \times D - 2.929\,\Delta z \times \Delta z - 5.75\,\mu \times \mu + 0.582\,D \\ & \times \Delta z - 0.006\,D \times \mu - 4.42\,\Delta z \times \mu\end{aligned} \quad (3)$$

$$\delta_s = 1.225 - 0.376\,D + 9.89\,\Delta z + 3.25\,\mu + 0.0290\,D \times D - 2.072\,\Delta z \times \Delta z - 15.72\,\mu \times \mu - 0710\,D \times \Delta z + 0.020\,D \times \mu + 15.76\,\Delta z \times \mu \quad (4)$$

The analysis of variance (ANOVA) of the three geometric errors was conducted, as an integral part of RSM study, to determine the effects of punch diameter, step size and friction coefficient as well as the effects of their interactions on the responses. This statistical analysis technique was carried out using the commercial software Minitab 17.

Additionally, for further illustration of accuracy of the developed model, the scatter plots between the predicted and actual values for bending error $(\boldsymbol{\delta_b})$, pillow effect error $(\boldsymbol{\delta_p})$ and springback error $(\boldsymbol{\delta_s})$ were drawn during this study. As it can be observed from Fig. 5, residuals for the studied responses are verified to follow a normal distribution assumption, considering an approximately straight-line distribution. The obtained models in Eqs. (2), (3) and (4) are thus served as a very good base in order to determine the optimal forming parameters.

Figure 6 presents the main effect plots for three process responses: bending error $(\boldsymbol{\delta_b})$, pillow effect error $(\boldsymbol{\delta_p})$ and springback error $(\boldsymbol{\delta_s})$. Comparing the impacts of the process factors: tool diameter (D), incremental step size (Δz) and friction coefficient (μ) on these above mentioned responses, it can be noted that changes carried out between the low and high levels of different parameters affect, more or less, the variation of the response. According to Fig. 6, the vertical increment (Δz) seems to be the most influencing factor on the springback and pillow effect errors while the punch diameter (D) has more influence on the bending error. However, the friction coefficient (μ) is the factor with much less important effects on the responses. As can be seen in Fig. 6c, a variation of Δz from 0.02 to 0.2 mm leads to an amplification of the springback error from 0.33 to 0.76 mm. The graphs of the main effects emphasize immediately the significant factors.

Based on the preceding results, the RSM can be used to construct the global approximation of the responses at various sampled points of design space. Figure 7 shows an example of three-dimensional representation of the relative variation of the predicted bending error $(\boldsymbol{\delta_b})$, pillow effect error $(\boldsymbol{\delta_p})$ and springback error $(\boldsymbol{\delta_s})$ given in the form of surface and contour plots. Due to its low effect, the friction coefficient (μ) can be fixed to its medium value. The results

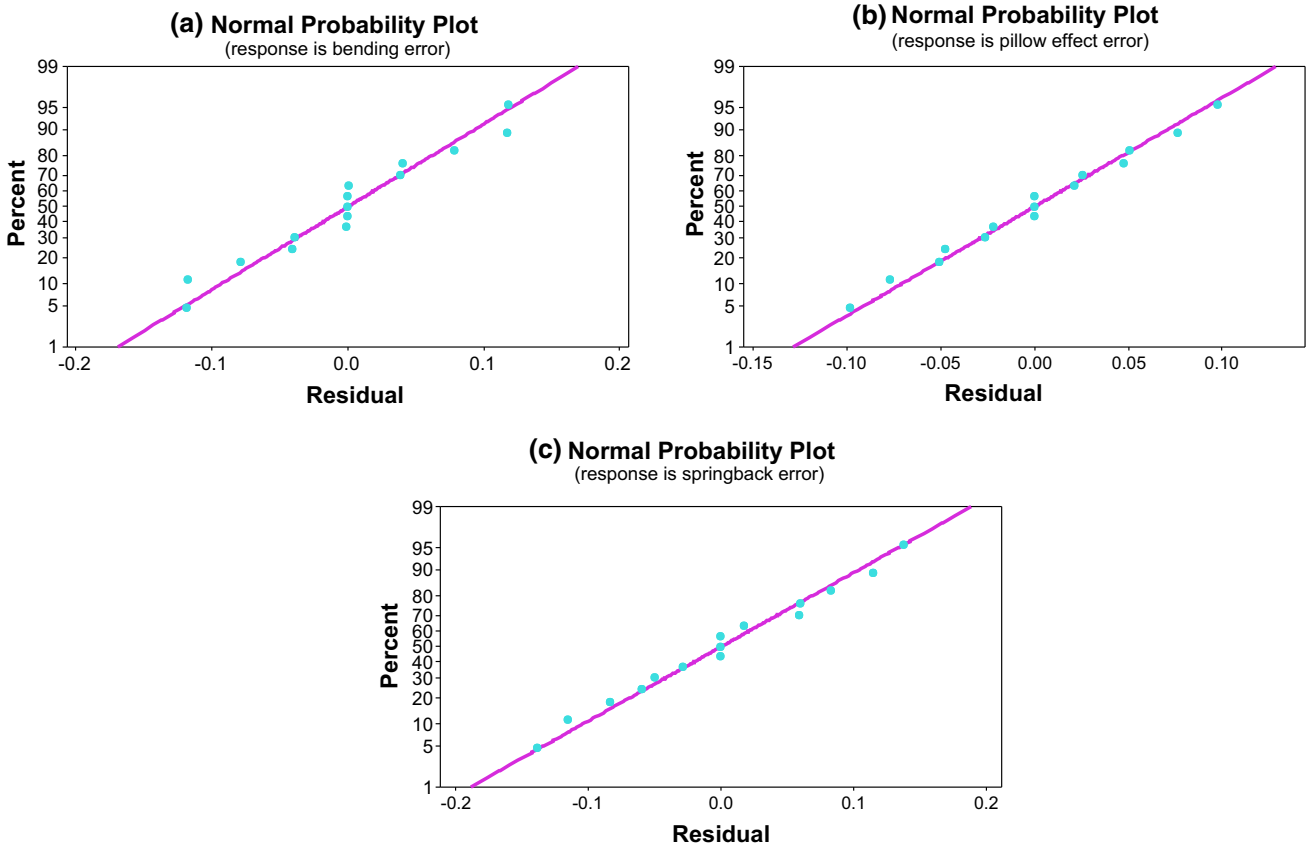

Fig. 5 Normal probability plots of the residuals for the three responses, respectively, **a** bending error $(\boldsymbol{\delta_b})$, **b** pillow effect error $(\boldsymbol{\delta_p})$ and **c** springback error $(\boldsymbol{\delta_s})$

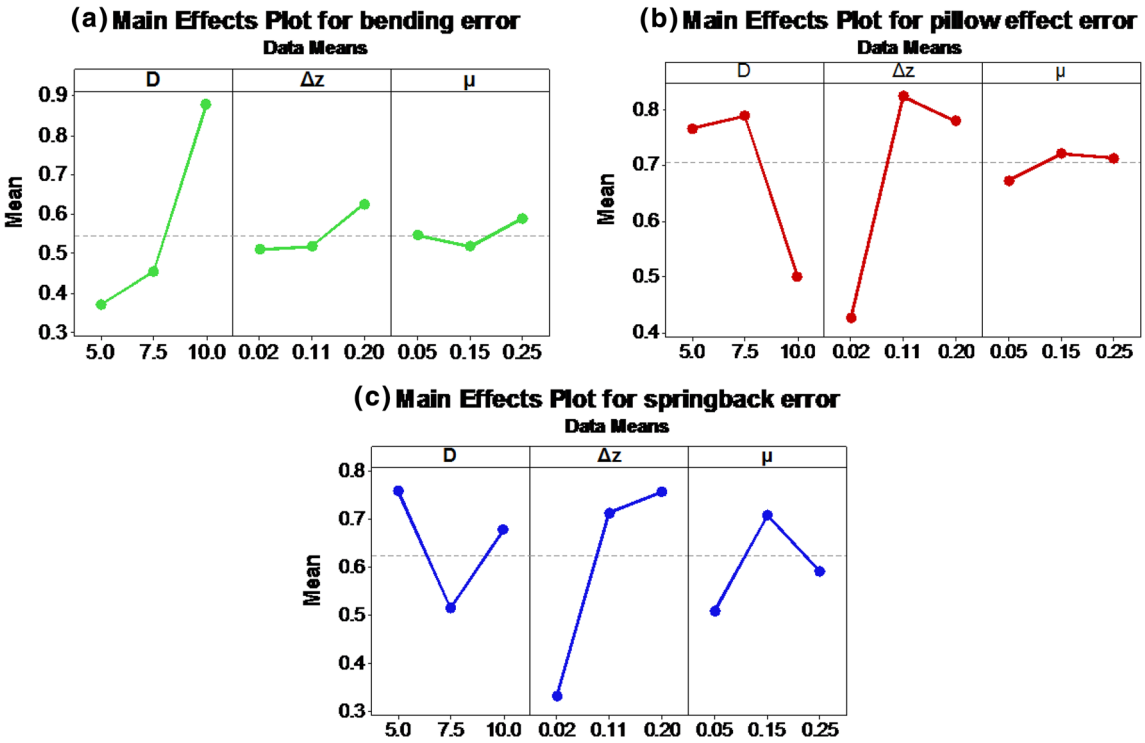

Fig. 6 Main effect plots of the three studied process parameters for: **a** bending error (δ_b), **b** pillow effect error (δ_p) and **c** springback error (δ_s)

show that the process responses evolve in a nonlinear way according to the considered parameters (D, Δz).

It can be evoked from Fig. 7a$_i$, that the variations of the last two responses pillow effect error (δ_p) and springback error (δ_s) are more sensitive to the vertical step size than to the punch diameter. These corresponding figures show that the increase in the vertical increment step size represents an amplification of these geometrical errors.

4 Optimization algorithms for the minimization of geometric errors in SPIF process

Once the response surface is constructed for the considered process outputs, the optimization problems will be solved using the following described algorithms for searching the decisions variables leading to optimal solutions of continuous nonlinear optimization problems.

4.1 Genetic algorithms

Genetic algorithms (GAs) are optimization techniques that are inspired by the basic principles of selection, evolution and inheritance in nature or by Darwin's theory of survival of the fittest [58]. The basic elements of natural genetics such as the reproduction, the crossover and the mutation are used in the genetic search procedure. GAs are a heuristic techniques particularly well suited using stochastic optimization that simulates natural evolution on the solution space of the optimization problems. This type of method is highly capable to find the global optimum solution (minimum or maximum of a function) by searching the space with a high probability. The data processed by GA include a set of chromosomes with an infinite length in which each bit is called a gene. A selected number of strings are called a population, and each population created during all processing time is also named a generation. In the initialization step, an initial population of strings is generated randomly. In our case, a binary encoding scheme is traditionally adopted to represent the chromosomes using either zeros or ones, since the binary coding offers the maximum number of schemata per bit of information. Thereafter, the fitness value of each member will be evaluated. The population is then operated by the three main operators, namely: selection, crossover, and mutation to create a new population. The new population is further computed and stopping criteria testing the convergence of genetic algorithm toward an optimal solution is used. One iteration after the application of these three operators is known as a generation in the parlance of GA.

GAs have been successfully applied to large optimization problems in various research areas such as engineering design, process planning, assembly and transportation problems, image processing, and scheduling. In this particular case, the GAs will be used as powerful tool for the

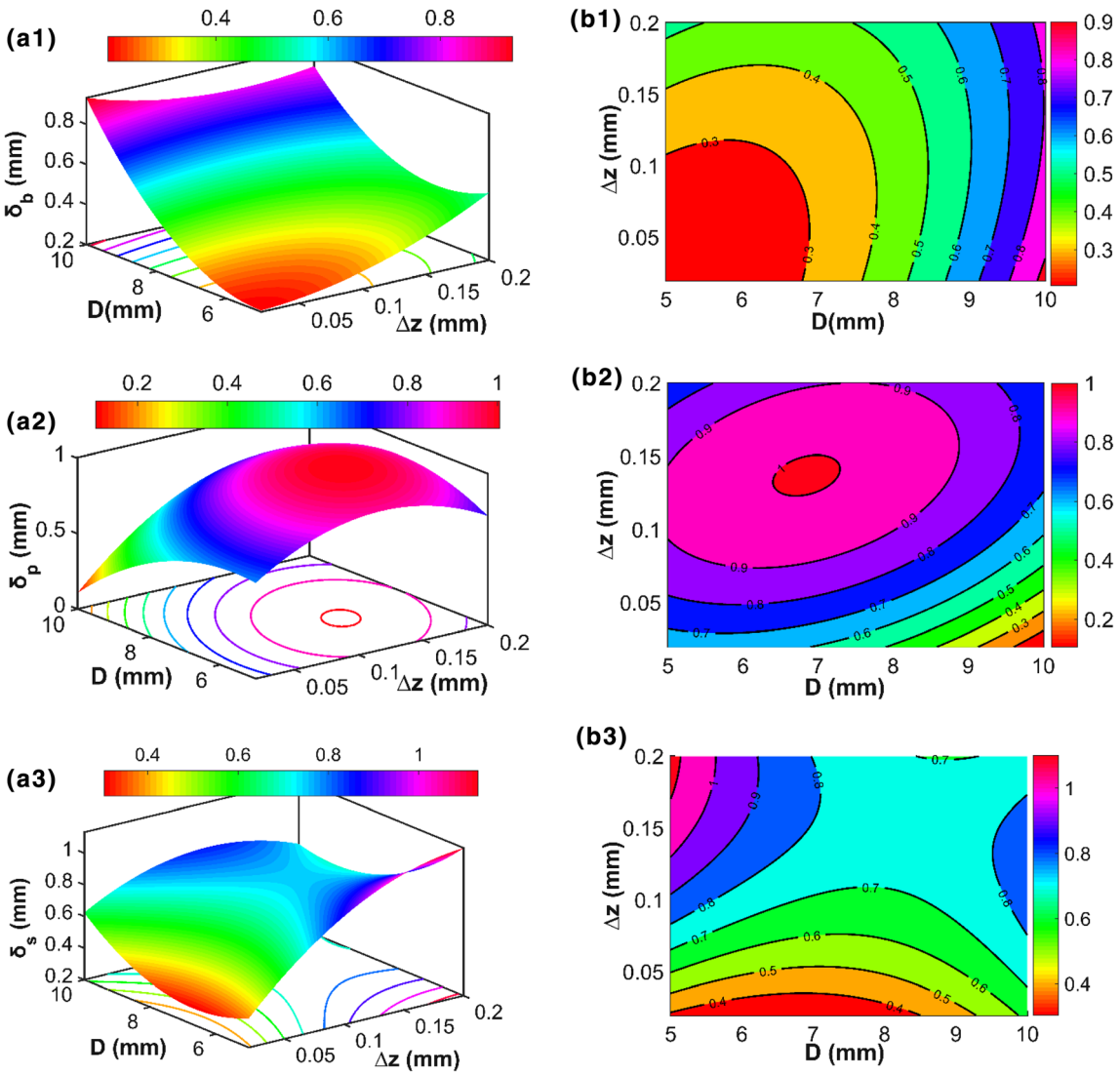

Fig. 7 Global evolution of bending error (δ_b), pillow effect error (δ_p) and springback error (δ_s) according to the punch diameter and the incremental step size for a constant value of friction coefficient ($\mu = 0.15$): $\mathbf{a_i}$ second order response surface and $\mathbf{b_i}$ contour plots

optimization of the incremental forming process parameters. The mono- and multi-objective genetic algorithm developed in the frame of our research works follow the steps outlined in the flowchart of Fig. 8.

4.2 Multi-objective genetic algorithm

The multi-objective genetic algorithm (MOGA) [59] is an extension of the classical GA that explicitly used Pareto-based ranking and niching techniques together to encourage the search toward the true Pareto front while maintaining diversity in the population. The main difference between a conventional GA and a MOGA resides in the assignment of fitness to an individual [60]. The rest of the algorithm is the same as that in a classical GA. MOGA is very attractive due to its capability to explore a larger extension of the design space and to compute multiple independent objective functions simultaneously in one optimization run. For these reasons, MOGA can be used for higher nonlinear MOOPs such as sheet metal forming.

Let $P(g)$ and $O(g)$ be parents and offspring in current generation g. The general structure of multi-objective genetic algorithm (MOGA) [61] can be described as follows (Fig. 9):

4.3 Global optimum determination by linking and interchanging kindred evaluators algorithm

In this contribution the "Global optimum determination by linking and interchanging kindred evaluators" (GODLIKE) [37, 62, 63] was used to optimize the geometrical errors

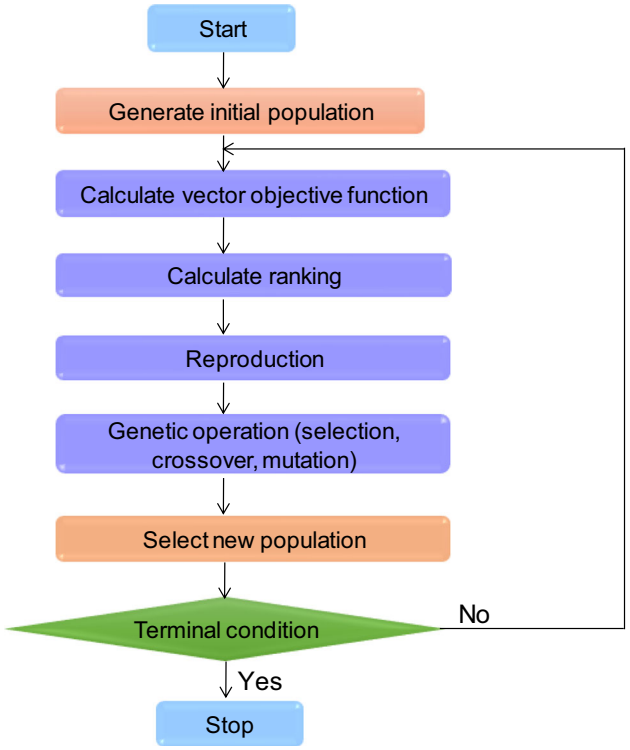

Fig. 8 Flowchart of the employed GA

predicted in SPIF process and to present the results in form of Pareto optimal frontier (POF). Figure 10 shows graphically the basic operations of GODLIKE solver. Thus, this algorithm solves optimization problems using relatively basic implementations of genetic algorithm (GA), differential evolution (DE), particle swarm optimization (PSO) and adaptive simulated annealing (ASA). GODLIKE is primarily intended to improve the robustness of the optimization method by exploiting the simultaneous running of the involved algorithms to decrease the chance of premature convergence to a local solution and to diminish the influence of the fine-tuning of each algorithm on the final solution. By using several optimizers at the same time, this amounts to performing four (or more) consecutive optimizations all at once, which already improves the chances of finding the global optimum. The weaknesses associated with each of these cited algorithms are neglected by the strengths and the performance of another, while the robustness of all algorithms simply adds up simultaneously. GODLIKE does not aim to make either of the algorithms more efficient in terms of function evaluations.

4.4 Grasshopper optimization algorithm

Grasshopper optimization algorithm (GOA) is one of the recent algorithms for optimization proposed by Saremi et al. [64]. This algorithm is swarm-based nature-inspired algorithm which mimics and mathematically models the swarming behavior of grasshoppers in nature. A mathematical model was proposed to simulate repulsion and attraction forces between the grasshoppers [64–66]. Repulsion forces allow grasshoppers to explore the search space, whereas attraction forces encouraged them to exploit promising regions. To balance between exploration and exploitation, GOA was equipped with a coefficient that adaptively decreases the comfort zone of the grasshoppers. Finally, the best solution obtained so far by the swarm was considered as a target to be chased and improved by the grasshoppers. The proposed mathematical model for the

Fig. 9 Pseudocodes of the MOGA algorithm [61]

***procedure**: MOGA*
***input**: problem data, GA parameters*
***output**: Pareto optimal solutions E*
begin
g ← 0;
initialize P(g) by encoding routine; calculate objectives fi(P),i = 1,⋯,q by decoding routine; create Pareto E(P); evaluate eval(P) by fitness assignment routine;
while** (**not** terminating condition) **do
    create O(g) from P(g) by crossover routine;
    create O(g) from P(g) by mutation routine;
    calculate objectives fi(O),i = 1,⋯,q by decoding routine;
    update Pareto E(P,O);
    evaluate eval(P,O) by fitness assignment routine;
    select P(g +1) from P(g) and O(g) by selection routine;
    g ← g +1;
end
***output** Pareto optimal solutions E(P,O)*
end

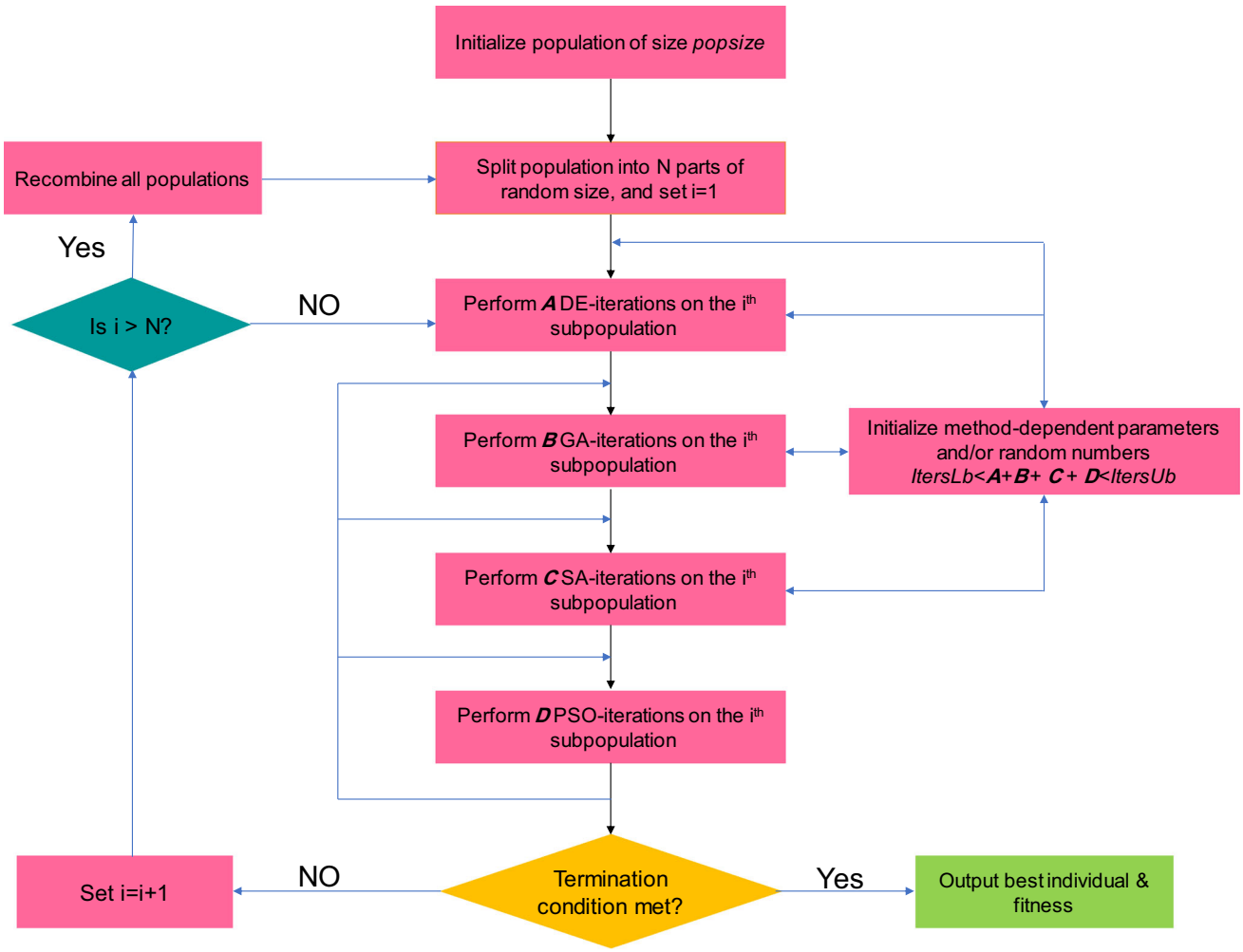

Fig. 10 Flowchart of the used GODLIKE hybrid algorithm [36]

simulation of the swarming behavior of grasshoppers is presented as follows:

$$X_i^d = c\left(\sum_{\substack{j=1\\ j\neq i}}^{N} c\frac{\mathrm{ub}_d - \mathrm{lb}_d}{2} s\left(\left|x_j^d - x_i^d\right|\right)\frac{x_j - x_i}{d_{ij}}\right) + \hat{T}_d \qquad (5)$$

where

- X_i^d defines the position of the ith grasshopper in the Dth dimension,
- N is the number of grasshoppers,
- ub_d and lb_d are, respectively, the upper and the lower bound in the Dth dimension,
- s defines the social forces: It represents how it impacts on the social interaction (attraction and repulsion) of grasshopper.
- $\hat{T}_d$ is the value of the Dth dimension in the target (best solution found so far),
- c is a decreasing coefficient to shrink the comfort zone, repulsion zone and attraction zone.

Equation (5) shows that the next position of a grasshopper is defined based on its current position, the position of the target and the position of all other grasshoppers.

For balancing exploration and exploitation, the parameter c is required to be decreased proportional to the number of iterations. This mechanism promotes exploitation as the iteration count increases. The coefficient c reduces the comfort zone proportional to the number of iterations and is calculated as follows:

$$c = c_{\max} - l\frac{c_{\max} - c_{\min}}{L} \qquad (6)$$

where $c_{\max}$ is the maximum value, $c_{\min}$ is the minimum value, l indicates the current iteration, and L is the maximum number of iterations. The pseudocode of the GOA algorithm is shown in Fig. 11.

Fig. 11 Pseudocodes of the GOA algorithm [48]

```
Initialize the swarm X_i (i= 1, 2, ..., n)
Initialize c_max, c_min, and maximum number of iterations
Calculate the fitness of each search agent
T= the best search agent
While (l < Max number of iterations)
    Update c using Eq. (6)
    for each search agent
        Normalize the distance between grasshoppers
        Update the position of the current search agent by the equation (5)
        Bring the current search agent back if it goes outside the boundaries
    end for
    Update T if there is a better solution
    l = l + 1
end while
Return T
```

The proposed algorithm can be used for solving the engineering optimization problems [64, 65]. In the next section, the possibility of application in real life of grasshopper optimization algorithm performances will be presented in our case of study.

4.5 Single-objective optimization problem

The fitness functions to minimize in this section are: the bending error $(\boldsymbol{\delta_b})$, the pillow effect error $(\boldsymbol{\delta_p})$ and the springback error $(\boldsymbol{\delta_s})$. Optimization is carried out in the search range of punch diameter (D) and vertical step size (Δz) in order to determine the optimal values of these process parameters guaranteeing the minimization of the considered process responses. So, the single-objective optimization problems (SOOP) could be formulated in the following form:

$$\text{Minimize } \delta_b = F_1(D, \Delta z, \mu) \tag{7a}$$

$$\text{Minimize } \delta_p = F_2(D, \Delta z, \mu) \tag{7b}$$

$$\text{Minimize } \delta_s = F_3(D, \Delta z, \mu) \tag{7c}$$

subject to the following inequality and equality constraints:

$$D_{\min} \le D \le D_{\max} \quad D \in [5\,\text{mm} \text{ to } 10\,\text{mm}] \tag{8a}$$

$$\Delta z_{\min} \le \Delta z \le \Delta z_{\max} \quad \Delta z \in [0.02\,\text{mm} \text{ to } 0.2\,\text{mm}] \tag{8b}$$

$$\mu = \text{constant value} \quad \mu = 0.15 \tag{8c}$$

In this section, the first tested method to solve the SOOP is the optimization with GA. Figure 12 presents the evolution of the cost function values versus the cumulated generations number for the responses $(\boldsymbol{\delta_b})$, $(\boldsymbol{\delta_p})$ and $(\boldsymbol{\delta_s})$, respectively. As reported in the representative curves, it can be noticed that the objective functions decrease rapidly during the first generations, and then the minimal values of these studied responses begin to be stable after the first twenty-five iterations until reaching the convergence toward their optimal solutions. According to Fig. 12a–c, the best solutions characterizing the minimum values of the objective functions are: $\boldsymbol{\delta_b}$-min = 0.207012, $\boldsymbol{\delta_p}$-min = 0.107249 and $\boldsymbol{\delta_s}$-min = 0.303145.

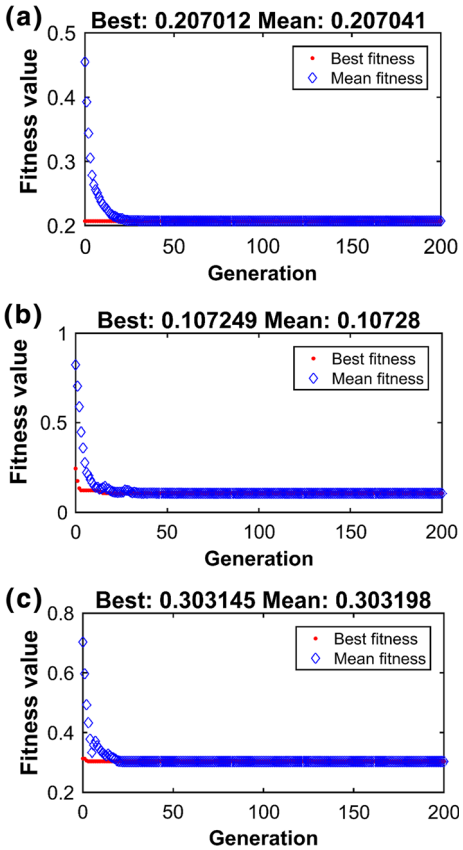

Fig. 12 Evaluation of fitness functions: **a** bending error (δ_b), **b** pillow effect error (δ_p) and **c** springback error (δ_s) with genetic algorithm versus cumulated number of generations

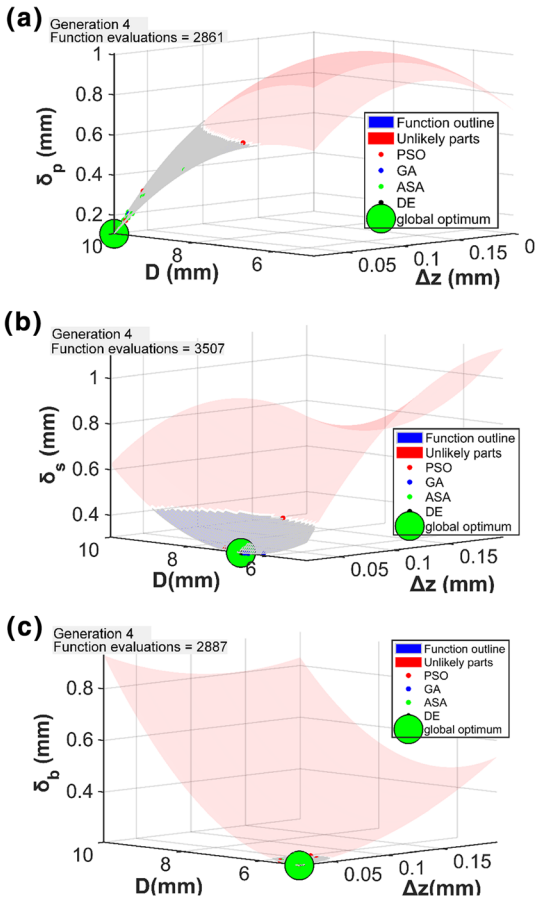

Fig. 13 Single optimization results: **a** bending error $(\boldsymbol{\delta_b})$, **b** pillow effect error $(\boldsymbol{\delta_p})$ and **c** springback error $(\boldsymbol{\delta_s})$ provided with GODLIKE optimizer approach

The same process responses have been optimized using the previously described GODLIKE mono-objective optimization evolutionary algorithm. As shown in Fig. 13a, b, c, the global optimal solution for each objective function has been extracted from the results of the optimized responses. The obtained optimized responses with GODLIKE solver for bending error, pillow effect error and springback error are: $\boldsymbol{\delta_b}$-min = 0.207000, $\boldsymbol{\delta_p}$-min = 0.107300 and $\boldsymbol{\delta_s}$-min = 0.303100, respectively.

Verification and validation of computer simulation models are performed by comparing these optimal results obtained through GODLIKE optimization algorithm with the previous one resulting from the integration of GA. Therefore, it can be clearly observed that the global minimums of different objective functions considered in this work are in very close agreement, which will make it possible the confirmation of the effectiveness and the reliability of these GODLIKE and GA-based optimization processes.

The main objective behind conducting this experiment was to observe the GOA algorithm behavior qualitatively [65]. Three diagrams have been drawn for each of the desirability function (Fig. 14):

- *Convergence curves* this diagram shows the objective value of the best solutions obtained so far (target) in each iteration.
- *Average fitness of grasshoppers* this diagram indicates the average objective value of all grasshoppers in each iteration.
- *Search history* this diagram shows the location history of the artificial grasshoppers during optimization.

The different curves presented in both Fig. 14a_i, b_i clearly show descending behavior on all of the objective functions. They have shown the advantageous of rapid convergence properties of grasshopper optimization algorithm toward the minimal value of all responses and for a small number of iterations. This proves that GOA enhances the initial random population on the cost functions and desirably improves the accuracy of the approximated optimum over the course of iterations.

It is worth noting from Fig. 14c_i that the grasshoppers tend to explore the different regions of the search space around the global optima eventually. These results will confirm that the GOA algorithm beneficially balances exploration and exploitation to drive the grasshoppers toward the global optimum.

In order to make a comparative study between all results determined by different optimization techniques, we chose to recapitulate in the same table all optimal solution obtained and the corresponding design variables. The optimal process responses of the three fitness functions bending error, pillow effect error and springback error obtained with GOA, GA and GODLIKE algorithms have been summarized in Table 2. The deduced values of optimal process parameters denoted by (D_opt) and (Δz_opt) are also presented for comparison. According to these results, it was found that the three tested algorithms lead approximately to the same response value of for each objective function. From Table 2, it can also be seen that the global optimum computed by all methods is obtained for almost identical design points characterized by same values of incremental step depth and for slightly different tool diameters. Consequently, these results can thus be observed as satisfactory.

Another important remark concerns the presence of antagonistic and non-comparable objective functions. In fact, an overall optimal solution corresponding to the best geometrical accuracy minimum with respect to minimum bending and springback errors during the SPIF operation and involving smaller size of punch diameter but higher value is automatically attained when minimizing pillow effect error. To resolve this problem of conflicting relations, a multi-criteria optimization and

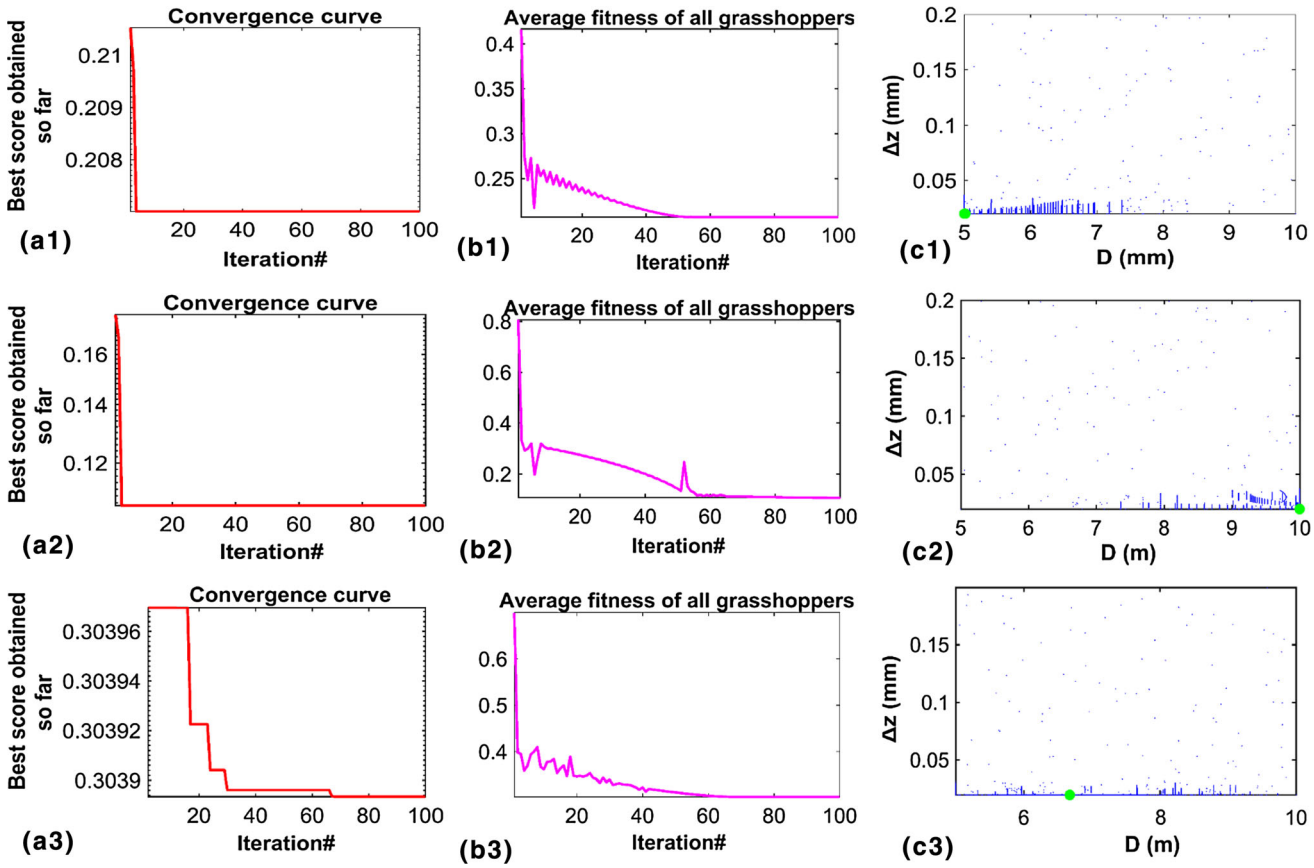

Fig. 14 Single optimization results in SPIF process with GOA for bending error (δ_b), pillow effect error (δ_p) and springback error (δ_s), respectively: $\mathbf{a_i}$ convergence curves, $\mathbf{b_i}$ average fitness of all grasshoppers and $\mathbf{c_i}$ exploration of the search space and localization of the global optimum

decision-making technique by the use of multi-objective versions of these algorithms will be proposed and developed in the next section. It is considered as efficiency methodology and a better way to solve an engineering optimization problem.

4.6 Tri-objective optimization problems

The multi-objective optimization technique [67] will be used to search the optimal solutions for the three considered process outputs simultaneously. A generic formulation of the multi-objective optimization problems (MOOP) can be defined by the following equations:

$$\begin{cases} \text{Minimize} & \vec{y} = \vec{F}(\vec{X}) = \left[f_1(\vec{X}), f_2(\vec{X}), \ldots, f_N(\vec{X})\right]^T \\ \text{Subject to} & g_i(\vec{X}) \le 0, \quad i = 1, 2, \ldots, m \\ & h_j(\vec{X}) \le 0, \quad j = 1, 2, \ldots, l \\ \text{Where} & \vec{X} = \left[X_1, X_2, \ldots, X_p\right)]^T \in \Omega \\ & X^L \le X \le X^U \end{cases} \tag{9}$$

where $\vec{y}$ is the objective vector, is a vector with the values of scalar objective functions to be minimized, m and l represent, respectively, the number of inequality, $g_i(\vec{X})$, and equality, $h_j(\vec{X})$. $\vec{X}$ is a P-dimensional vector

Table 2 Summary table of different optimization results corresponding to the minimization of bending error, pillow effect error and springback error obtained by three optimization methods

Objective functions	Bending error (δ_b)			Pillow effect error (δ_p)			Springback error (δ_s)		
Optimization methods	GA	GODLIKE	GOA	GA	GODLIKE	GOA	GA	GODLIKE	GOA
Global minimum	0.207012	0.207000	0.20701	0.107249	0.107300	0.10725	0.303145	0.303100	0.30315
(D_opt)	5.008	5.0082	5.0083	10	9.9999	10	6.676	6.6817	6.6759
(Δz_opt)	0.02	0.02	0.02	0.02	0.02	0.02	0.02	0.02	0.02

representing the decision variables within a parameter space Ω. X^L and X^U are the lower and upper bound vectors of the design parameters X.

The tri-objective optimization design of SPIF can offer more choices for a designer. This will allow us to find trade-off optimum design points allowing to minimize all three objective functions of bending $(\boldsymbol{\delta_b})$, pillow effect $(\boldsymbol{\delta_p})$ and springback $(\boldsymbol{\delta_s})$ errors, simultaneously. The multi-criteria optimization system in single point incremental forming problem can be formulated in the following form:

$$\text{Minimize} \begin{cases} \delta_b = F_1(D, \Delta z, \mu) \\ \delta_p = F_2(D, \Delta z, \mu) \\ \delta_s = F_3(D, \Delta z, \mu) \end{cases} \tag{10}$$

subject to the common conditions of inequality and equality constraints, given below:

$$\begin{cases} 5\,\text{mm} \le D \le 10\,\text{mm} \\ 0.02\,\text{mm} \le \Delta z \le 0.2\,\text{mm} \\ \mu = 0.15 \end{cases} \tag{11}$$

Figure 15 shows the final Pareto of the optimal responses obtained with the multi-objective genetic algorithm (MOGA) method and the GODLIKE solver. As it can be noted from Fig. 15a, the obtained Pareto optimal design of SPIF process using MOGA routine can offer several optimal solutions. With GODLIKE solver, unique solution presented by the green dot in the final Pareto plot (Fig. 15b) is corresponding to the most efficient point of the MOOP.

Table 3 summarizes the optimal process parameters combinations of the studied problem obtained with MOGA. The optimization results given by GODLIKE in terms of the most efficient solution are illustrated in Table 4. According to these tables, it can be seen that the optimal solution: $D \approx 8$ mm and $\Delta z \approx 0.02$ mm is a common solution between both studied multi-objective algorithms. Therefore, for the validation of these results described numerically, experimental tests will be done based on the obtained value of optimum process parameters.

5 Experimental validation

Experiments were carried out using Amino DLNC-RB machine to manufacture the denture base. The previously chosen combination of optimal process parameters obtained with multi-objective optimization approach was employed for practical test. It corresponds to tool diameter value of $D = 8$ mm and incremental step down Δz equal to 0.02 mm. In order to reduce the friction phenomenon and obtain a better formability of material, chlorine-containing forming oils were applied as a lubricant. Figure 16 illustrates the experimental test conducted in single point

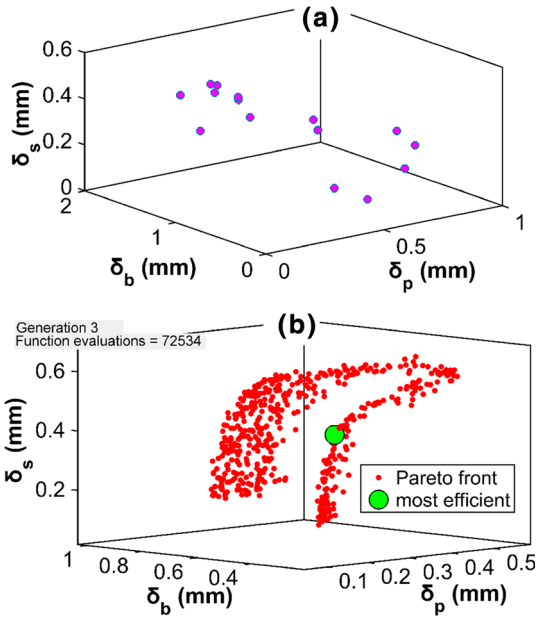

Fig. 15 Tri-objective optimization results with **a** MOGA and **b** GODLIKE algorithms

incremental forming process to experimentally verify the efficacity of the optimization strategy. The metal sheet used for SPIF process was made of Commercially Pure Grade 1 Titanium.

Moreover, the measured geometry of the formed denture base made by SPIF technology is obtained from an 3D optical measuring system GOM ATOS. As depicted in Fig. 17, a cross-sectional comparison among deformed profile and the target profile representing the desired

Table 3 Optimal process parameters calculated by MOGA algorithm

D (mm)	Δz (mm)
5.00976563	0.02000095
9.98118211	0.0200931
6.6629387	0.02001164
8.21687672	0.02078405
8.01577028	0.02007967
9.98118211	0.0200931
6.25703032	0.02465748
8.4338668	0.02169529
9.22629428	0.02019992
8.98496061	0.02085449
8.52908391	0.0204045
9.14430126	0.02266056
8.8242337	0.02210532
8.80944024	0.02506461
9.62526478	0.02074483
9.21680786	0.02106186
9.46697476	0.02429296
7.51057595	0.02382012

Table 4 Efficient solution to a multiple objective optimization problem computed by GODLIKE solver

Optimal solutions (δ_b, δ_p, δ_s)	Optimal factors (D, Δz)
(0.4684, 0.4858, 0.3549)	(8.0106, 0.0200)

original CAD model was conducted. In particular, Fig. 17b reports the topographic map of the geometrical error and its frequency distributions. The error distributions are compared in terms of average value and uniformity. As it can be observed from these two presented figures, the most critical zones containing the maximum errors are located in the upper boundaries (due to the bending effect) and in the central region of the bottom of the part (due to the pillow effect). In fact, the zones on boundary are the farthest from the punch and the closest to the backing plate and, therefore, they are subjected to more severe bending stresses during forming. In the studied case, the error map is generally symmetric and seems to be uniform. Therefore, the error fluctuation varies in an interval which does not exceed in any case 0.4 mm, judged to be satisfactory. In conclusion, the optimization methods help to compensate the previously described errors without losing time and material on the experimental tests.

6 Conclusion

The presented work deals with one of the main drawbacks of the SPIF process which is the low geometrical accuracy achievable on the workpiece due to different phenomena like springback, sheet bending and pillow effect. During these research studies, we are concentrated on the assessment of the geometrical quality for biomedical parts fabricated by incremental forming technology, in order to improve the process in terms of desired dimensional accuracy achievement. For doing that an optimization study has been consequently performed for geometrical errors compensation. It consists of proving its capability for a particular studied case for biomedical application, in particular, for a denture plate. Based on the noted errors in our previous research works, the precision of ISF product has been controlled and enhanced within a parameterized numerical model based on the finite element method (FEM) and different optimization algorithms.

This experiment and relevant discussions support the following conclusions:

- The results show that the different implemented numerical optimization algorithms are able to provide superior results.
- The results of the real applications also prove the merits of the recent grasshopper optimization algorithm (GOA) considered as a modern high-performance algorithm for solving real problems compared with other classical algorithms more known in the literature, such as GA and GODLIKE.
- For multi-objective optimization results, it can be deduced that MOGA and GODLIKE techniques lead to one common optimal solution.

The obtained optimal parameters, applied in experimental test of SPIF process, help to compensate the

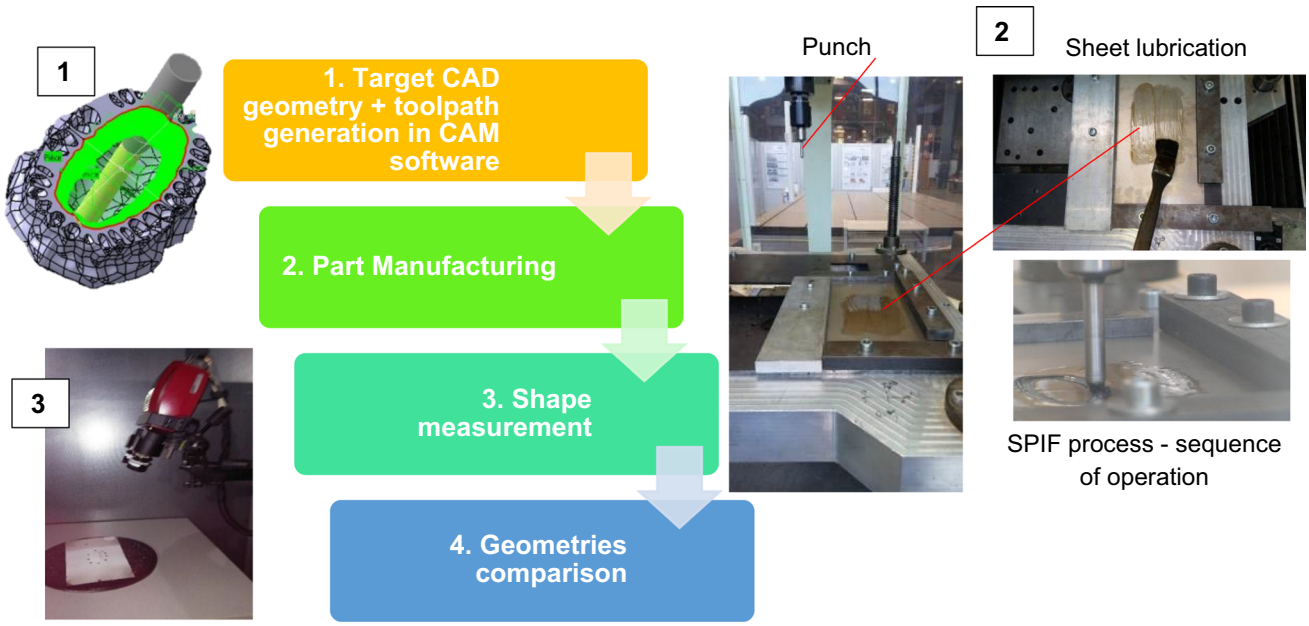

Fig. 16 Experimental procedure and single point incremental forming setup at the institute of metal forming of RWTH Aachen University

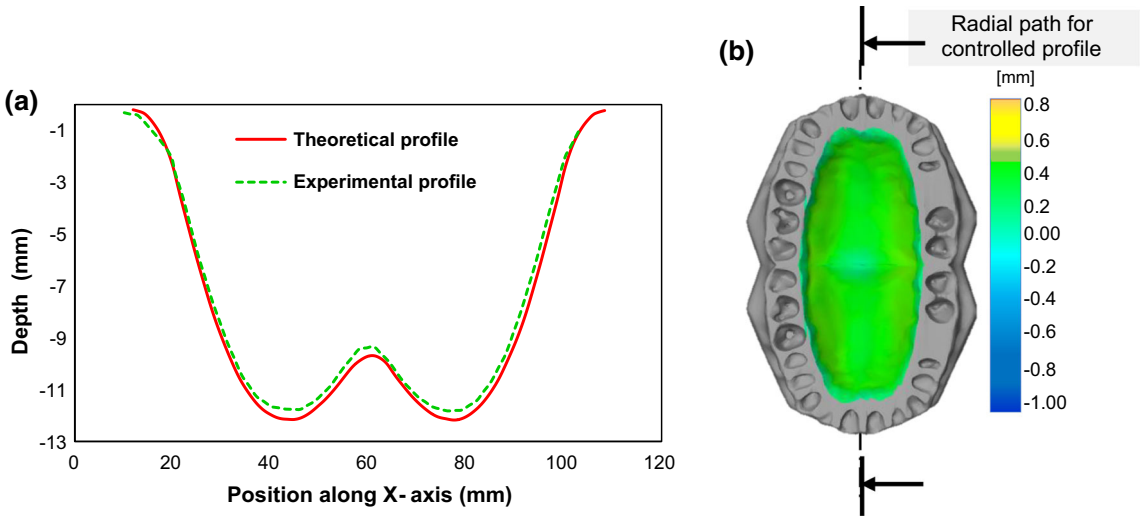

Fig. 17 **a** Comparison of the geometry profile obtained experimentally by SPIF with original CAD part profile scanned from real prosthesis of denture plate, **b** topographic map characterizing the frequency distributions of the geometrical error

geometrical errors. By analyzing part geometry with 3D optical measurement system, geometrical precision achievement has been noted. This proves the capabilities of the presented optimization strategy. Compared to majority of last works for geometric accuracy enhancement in SPIF which are based on several experimental tests, this study has an economic aspect.

Acknowledgements The authors would like to thank the Faculty of Dental Medicine of Monastir, Tunisia for providing the original denture plate prosthesis and the German Research Foundation DFG for the kind support within the Cluster of Excellence "Integrative Production Technology for High-Wage Countries." Furthermore, the authors thank the Institute of Metal Forming of RWTH Aachen University for their support in the performance and evaluation of the incremental sheet forming experiments.

Compliance with ethical standards

Conflict of interest Authors declare that they do not have any commercial or associative interest that represents a conflict of interest in connection with the work submitted.

References

1. Schuh G, Prote J, Dany S, Cremer S, Molitor M (2017) Classification of a hybrid production infrastructure in a learning factory morphology. Proc Manuf 9:17–24. https://doi.org/10.1016/j.promfg.2017.04.007
2. Ambrogio G, De Napoli L, Filice L, Gagliardi F, Muzzupappa M (2005) Application of incremental forming process for high customised medical product manufacturing. J Mater Process Technol 162–163:156–162. https://doi.org/10.1016/j.jmatprotec.2005.02.148
3. Boulila A, Ayadi M, Marzouki S, Bouzidi S (2017) Contribution to a biomedical component production using incremental sheet forming. Int J Adv Manuf Technol 95(5–8):2821–2833. https://doi.org/10.1007/s00170-017-1397-4
4. Sbayti M, Ghiotti A, Bahloul R, Belhadjsalah H, Bruschi S (2016) Finite element analysis of hot single point incremental forming of hip prostheses. MATEC Web Conf 80(14006):1–7. https://doi.org/10.1051/matecconf/20168014006
5. Hirt G, Ames J, Bambach M, Kopp R (2004) Forming strategies and process modelling for CNC incremental sheet forming. CIRP Ann Manuf Technol 53:203–206. https://doi.org/10.1016/S0007-8506(07)60679-9
6. Bahloul R, Arfa H, Belhadjsalah H (2011) Process analysis based on experimental tests and numerical modelling of single point incremental forming of sheet metal: effect of the principal process parameters. In: Proceedings of the XI international conference on computational plasticity (COMPLAS). Barcelona
7. Governale A, Lo Franco A, Panzeca A et al (2007) Incremental forming process for the accomplishment of automotive details. Key Eng Mater 344:559–566. https://doi.org/10.4028/www.scientific.net/KEM.344.559
8. Hussain G, Khan HR, Gao L, Hayat N (2013) Guidelines for tool-size selection for single-point incremental forming of an aerospace alloy. Mater Manuf Process 28(3):324–329. https://doi.org/10.1080/10426914.2012.700151
9. Lu B, Ou H, Shi SQ, Long H, Chen J (2016) Titanium based cranial reconstruction using incremental sheet forming. Int J Mater Form 9:361–370. https://doi.org/10.1007/s12289-014-1205-8
10. Araújo R, Teixeira P, Montanari L, Reis A, Silva MB, Martins PAF (2014) Single point incremental forming of a facial implant. Prosthet Orthot Int 38:369–378. https://doi.org/10.1177/0309364613502071
11. Castelan J, Schaeffer L, Daleffe A et al (2014) Manufacture of custom-made cranial implants from DICOM® images using 3D printing, CAD/CAM technology and incremental sheet forming. Rev Bras Eng Biomed 30:265–273. https://doi.org/10.1590/rbeb.2014.024
12. Duflou JR, Behera AK, Vanhove H, Bertol LS (2013) Manufacture of accurate titanium cranio-facial implants with high forming angle using single point incremental forming. Key Eng Mater 549:223–230. https://doi.org/10.4028/www.scientific.net/KEM.549.223
13. Fiorentino A, Marenda GP, Marzi R, Ceretti E, Kemmoku DT, Lopes da Silva JV (2012) Rapid prototyping techniques for individualized medical prosthesis manufacturing. In: Proceedings

of the 5th international conference on advanced research in virtual and rapid prototyping, vol 1, pp 589–594. https://doi.org/10.1201/b11341-94
14. Fiorentino A, Attanasio A, Marzi R, Ceretti E, Giardini C (2011) On forces, formability and geometrical error in metal incremental sheet forming. Int J Mater Prod Tec. https://doi.org/10.1504/IJMPT.2011.039936
15. Attanasio A, Ceretti E, Giardini C, Mazzoni L (2007) Asymmetric two points incremental forming: improving surface quality and geometric accuracy by tool path optimization. J Mater Process Technol 197:59–67. https://doi.org/10.1016/j.jmatprotec.2007.05.053
16. Li Y, Lu H, Daniel WJT, Meehan PA (2015) Investigation and optimization of deformation energy and geometric accuracy in the incremental sheet forming process using response surface methodology. Int J Adv Manuf Technol 79:2041–2055. https://doi.org/10.1007/s00170-015-6986-5
17. Taleb Araghi B, Manco GL, Bambach M, Hirt G (2009) Investigation into a new hybrid forming process: incremental sheet forming combined with stretch forming. CIRP Ann Manuf Technol 58:225–228. https://doi.org/10.1016/j.cirp.2009.03.101
18. Taleb Araghi B, Göttmann A, Bambach M, Hirt G, Bergweiler G, Diettrich J, Steiners M, Saeed-akbari A (2011) Review on the development of a hybrid incremental sheet forming system for small batch sizes and individualized production. Prod Eng Res Dev 5:393–404. https://doi.org/10.1007/s11740-011-0325-y
19. Ambrogio G, De Napoli L, Filice L (2009) A novel approach based on multiple back-drawing incremental forming to reduce geometry deviation. Int J Mater Form 2:9–12. https://doi.org/10.1007/s12289-009-0498-5
20. Allwood JM, Braun D, Music O (2010) The effect of partially cut-out blanks on geometric accuracy in incremental sheet forming. J Mater Process Technol 210:1501–1510. https://doi.org/10.1016/j.jmatprotec.2010.04.008
21. Bambach M, Taleb Araghi B, Hirt G (2009) Strategies to improve the geometric accuracy in asymmetric single point incremental forming. Prod Eng Res Dev 3:145–156. https://doi.org/10.1007/s11740-009-0150-8
22. Lu B, Chen J, Ou H, Cao J (2013) Feature-based tool path generation approach for incremental sheet forming process. J Mater Process Technol 213:1221–1233. https://doi.org/10.1016/j.jmatprotec.2013.01.023
23. Behera AK, Verbert J, Lauwers B, Duflou JR (2013) Tool path compensation strategies for single point incremental sheet forming using multivariate adaptive regression splines. CAD Comput Aided Des 45:575–590. https://doi.org/10.1016/j.cad.2012.10.045
24. Malhotra R, Bhattacharya A, Kumar A, Reddy NV, Cao J (2011) A new methodology for multi-pass single point incremental forming with mixed toolpaths. CIRP Ann Manuf Technol 60:323–326. https://doi.org/10.1016/j.cirp.2011.03.145
25. Behera AK, Lauwers B, Duflou JR (2015) Tool path generation for single point incremental forming using intelligent sequencing and multi-step mesh morphing techniques. Int J Mater Form 8:517–532. https://doi.org/10.1007/s12289-014-1174-y
26. Junchao L, Junjian S, Bin W (2013) A multipass incremental sheet forming strategy of a car taillight bracket. Int J Adv Manuf Technol 69:2229–2236. https://doi.org/10.1007/s00170-013-5179-3
27. Fu Z, Mo J, Han F, Gong P (2013) Tool path correction algorithm for single-point incremental forming of sheet metal. Int J Adv Manuf Technol 64:1239–1248. https://doi.org/10.1007/s00170-012-4082-7
28. Fiorentino A, Giardini C, Ceretti E (2015) Application of artificial cognitive system to incremental sheet forming machine tools for part precision improvement. Precis Eng 39:167–172. https://doi.org/10.1016/j.precisioneng.2014.08.005
29. Allwood JM, Music O, Raithathna A, Duncan SR (2009) Closed-loop feedback control of product properties in flexible metal forming processes with mobile tools. CIRP Ann Manuf Technol 58:287–290. https://doi.org/10.1016/j.cirp.2009.03.065
30. Hao W, Duncan S (2011) Constrained model predictive control of an incremental sheet forming process. In: IEEE international conference on control applications (CCA). https://doi.org/10.1109/CCA.2011.6044466
31. Lu H, Kearney M, Wang C, Liu S, Meehan PA (2017) Part accuracy improvement in two point incremental forming with a partial die using a model predictive control algorithm. Precis Eng 49:179–188. https://doi.org/10.1016/j.precisioneng.2017.02.006
32. Bahloul R, Arfa H, BelHadjSalah H (2014) A study on optimal design of process parameters in single point incremental forming of sheet metal by combining Box–Behnken design of experiments, response surface methods and genetic algorithms. Int J Adv Manuf Technol 74:163–185. https://doi.org/10.1007/s00170-014-5975-4
33. Bahloul R, Arfa H, BelHadjSalah H (2013) Application of response surface analysis and genetic algorithm for the optimization of single point incremental forming process. Key Eng Mater 554–557:1265–1272. https://doi.org/10.4028/www.scientific.net/KEM.554-557.1265
34. Ponthot JP, Kleinermann JP (2006) A cascade optimization methodology for automatic parameter identification and shape/process optimization in metal forming simulation. Comput Methods Appl Mech Eng 195:5472–5508. https://doi.org/10.1016/j.cma.2005.11.012
35. Ceretti E, Giardini C, Attanasio A (2004) Experimental and simulative results in sheet incremental forming on CNC machines. J Mater Proc Technol 152:176–184. https://doi.org/10.1016/j.jmatprotec.2004.03.024
36. Esmaeilpour R, Kim H, Park T, Pourboghrat F, Xu Z, Mohammed B, Abu-Farha F (2018) Calibration of Barlat Yld2004–18P yield function using CPFEM and 3D RVE for the simulation of single point incremental forming (SPIF) of 7075-O aluminum sheet. Int J Mech Sci 145:24–41. https://doi.org/10.1016/j.ijmecsci.2018.05.015
37. Sbayti M, Bahloul R, Belhadjsalah H, Zemzemi F (2018) Optimization techniques applied to single point incremental forming process for biomedical application. Int J Adv Manuf Technol 95:1789–1804. https://doi.org/10.1007/s00170-017-1305-y
38. Arfa H, Bahloul R, Belhadjsalah H (2015) Multiobjective optimization problem of dieless incremental forming. Key Eng Mater 651–653:1078–1083. https://doi.org/10.4028/www.scientific.net/KEM.651-653.1078
39. Khan MS, Coenen F, Dixon C, El-Salhi S, Penalva M, Rivero A (2015) An intelligent process model: predicting springback in single point incremental forming. Int J Adv Manuf Technol 76:2071–2082. https://doi.org/10.1007/s00170-014-6431-1
40. Isidore BBL, Hussain G, Shamchi SP, Khan WA (2016) Prediction and control of pillow defect in single point incremental forming using numerical simulations. J Mech Sci Technol 30:2151–2161. https://doi.org/10.1007/s12206-016-0422-0
41. Kumar PM, Gandhi UD (2017) Enhanced DTLS with CoAP-based authentication scheme for the internet of things in healthcare application. J Supercomput. https://doi.org/10.1007/s11227-017-2169-5
42. Kumar PM, Devi GU, Manogaran G, Sundarasekar R, Chilamkurti N, Varatharajan R (2018) Ant colony optimization algorithm with internet of vehicles for intelligent traffic control system. Comput Netw 144:154–162. https://doi.org/10.1016/j.comnet.2018.07.001

43. Kumar PM, Gandhi UD (2018) A novel three-tier internet of things architecture with machine learning algorithm for early detection of heart diseases. Comput Electr Eng 65:222–235. https://doi.org/10.1016/j.compeleceng.2017.09.001
44. Kumar PM, Lokesh S, Varatharajan R, Babu GC, Parthasarathy P (2018) Cloud and IoT based disease prediction and diagnosis system for healthcare using fuzzy neural classifier. Future Gener Comput Syst 86:527–534. https://doi.org/10.1016/j.future.2018.04.036
45. Varatharajan R, Manogaran G, Priyan MK, Balaş VE, Barna C (2018) Visual analysis of geospatial habitat suitability model based on inverse distance weighting with paired comparison analysis. Multimed Tools Appl 77:17573–17593. https://doi.org/10.1007/s11042-017-4768-9
46. Priyan MK, Devi GU (2018) Energy efficient node selection algorithm based on node performance index and random waypoint mobility model in internet of vehicles. Cluster Comput 21:213–227. https://doi.org/10.1007/s10586-017-0998-x
47. Manogaran G, Varatharajan R, Lopez D, Kumar PM, Sundarasekar R, Thota C (2018) A new architecture of internet of things and big data ecosystem for secured smart healthcare monitoring and alerting system. Future Gener Comput Syst 82:375–387. https://doi.org/10.1016/j.future.2017.10.045
48. Lokesh S, Kumar PM, Devi MR, Parthasarathy P, Gokulnath CB (2018) An automatic tamil speech recognition system by using bidirectional recurrent neural network with self-organizing map. Neural Comput Appl. https://doi.org/10.1007/s00521-018-3466-5
49. Pawlewski P (2012) Petri nets—manufacturing and computer science. IntechOpen Publisher, Rijeka. https://doi.org/10.5772/2578
50. Malhotra R, Cao J, Ren F, Kiridena V, Xia ZC, Reddy NV (2011) Improvement of geometric accuracy in incremental forming by using a squeezing toolpath strategy with two forming tools. J Manuf Sci Eng 133:061019. https://doi.org/10.1115/1.4005179
51. Malyer E (2013) The influence of toolpath strategy on geometric accuracy in incremental forming. Key Eng Mater 554–557:1351–1361. https://doi.org/10.4028/www.scientific.net/KEM.554-557.1351
52. Störkle DD, Seim P, Thyssen L, Kuhlenkötter B (2016) Influence of part orientation on the geometric accuracy in robot-based incremental sheet metal forming. AIP Conf Proc 1769:070002. https://doi.org/10.1063/1.4963455
53. Box GEP, Behnken DW (1960) Some new three level designs for the study of quantitative variables. Technometrics 2:455–475. https://doi.org/10.1080/00401706.1960.10489912
54. Bahloul R (2011) Optimisation of process parameters in flanging operation in order to minimise stresses and Lemaitre's damage. Mater Des 32(1):108–120. https://doi.org/10.1016/j.matdes.2010.06.028
55. Box GEP, Wilson KB (1951) On the experimental attainment of optimum conditions. J R Stat Soc 13:1–45
56. Petersen RG (1985) Design and analysis of experiments. Marcel Dekker Inc., New York
57. Roy K, Kar S, Narayan Das R (2015) A primer on QSAR/QSPR modeling: fundamental concepts. Springer, Berlin. https://doi.org/10.1007/978-3-319-17281-1
58. Goldberg DE (1989) Genetic algorithms in search, optimization, and machine learning. Addison-Wesley Longman Publishing Co., Inc., Boston
59. Fonseca CM, Fleming PJ (1993) Multiobjective genetic algorithm. In: Proceedings of IEE colloquium on genetic algorithms for control systems engineering, vol 6, pp 1–5 (Digest No. 1993/130). London
60. Fonseca CM, Fleming PJ (1995) An overview of evolutionary algorithms in multiobjective optimization. Evol Comput 3(1):1–16. https://doi.org/10.1162/evco.1995.3.1.1
61. Gen M, Cheng R (2000) Genetic algorithms and engineering optimization. Wiley, New York
62. Oldenhuis R (2017) GODLIKE—a robust single-& multi-objective optimizer—file exchange—MATLAB central. www.mathworks.it/matlabcentral/fileexchange/24838-godlike-a-robust-single-multi-objective-optimizer. Accessed 1 Jan 2017
63. Narkhede MS, Chatterji S, Ghosh S (2015) Comparative analysis of ev-moga and godlike multiobjective evolutionary algorithms for risk based optimal power scheduling of a virtual power plant. ICTACT J Soft Comput 5:917–924. https://doi.org/10.21917/ijsc.2015.0129
64. Saremi S, Mirjalili S, Lewis A (2017) Grasshopper optimisation algorithm: theory and application. Adv Eng Softw 105:30–47. https://doi.org/10.1016/j.advengsoft.2017.01.004
65. Neve AG, Kakandikar GM, Kulkarni O (2017) Application of grasshopper optimization algorithm for constrained and unconstrained test functions. Int J Swarm Intel Evol Comput 6(3):1–7. https://doi.org/10.4172/2090-4908.1000165
66. Saremi S, Mirjalili S, Mirjalili S, Dong JS (2020) Grasshopper optimization algorithm: theory, literature review, and application in hand posture estimation. In: Mirjalili S, Dong JS, Lewis A (eds) Nature-inspired optimizers. Studies in computational intelligence, vol 811. Springer, Cham, pp 107–122. https://doi.org/10.1007/978-3-030-12127-3_7
67. Aragón AM, Wayer JK, Geubelle PH, Goldberg DE, White SR (2008) Design of microvascular flow networks using multi-objective genetic algorithms. Comput Methods Appl Mech Eng 197(49–50):4399–4410. https://doi.org/10.1016/j.cma.2008.05.025